Prescribed position control, Acceleration profile, Velocity profile, Permanent magnet synchronous motor, Minimum energy generator, Zero dynamics lag pre-compensator, Energy expenditure

Peter MINÁRECH [1]
Ján VITTEK [1]
Elżbieta SZYCHTA [2]
Mirosław LUFT [2]

ENERGY SAVING PMSM POSITION CONTROL RESPECTING COULOMB FRICTION

The paper describes development of a new energy saving control algorithms for precise position control of permanent magnet synchronous motor. Designed control algorithms limit energy consumption for defined rotor position maneveur, increase efficiency of the drive and contribute to the substantial improvements of environment. Overall position control system consists of three parts. As the first part, the 'minimum energy generator' computes a special acceleration, velocity and position profile, where the magnitude and time of acceleration or deceleration are determined such a way that comply with position demand and prescribed time for position maneuver. The role of 'feed-forward precompensator', as a second part, is to achieve precise tracking of the prescribed reference position with zero dynamic lag. Third part is position controller, which can be based on field oriented control, forced dynamics control or sliding mode control. Developed 'energy saving control algorithms' are easy to implement digitally and can be exploited for position control of existing a.c. drives.

ENERGOOSZCZĘDNE STEROWANIE POŁOŻENIEM SILNIKA SYNCHRONICZNEGO Z MAGNESAMI TRWAŁYMI (PMSM) Z UWZGLĘDNIENIEM TARCIA COULOMBA

Artykuł opisuje wyznaczenie nowych algorytmów energooszczędnego sterowania do precyzyjnego sterowania położeniem silnika synchronicznego z magnesami trwałymi. Zaprojektowane algorytmy sterowania ograniczają zużycie energii dla określonego manewru położeniem wirnika, zwiększają efektywność napędu i przyczyniają się do istotnej poprawy środowiska. Ogólnie rzecz biorąc, system sterowania położeniem składa się z trzech części. Jako część pierwsza, „generator minimalnej energii" oblicza szczególne profile przyspieszenia, prędkości i położenia, gdzie wielkość i czas przyspieszenia lub deceleracji są wyznaczane w taki sposób, że są zgodne z żądanym położeniem i czasem przewidzianym na manewr zmiany położenia. Rolą „wstępnego kompensatora sprzężenia antycypacyjnego", jako drugiej części, jest osiągnięcie precyzyjnego namierzenia przewidzianego położenia referencyjnego (odniesienia) przy zerowym opóźnieniu dynamicznym. Trzecią częścią jest sterownik położenia, który może bazować zorientowanym sterowaniu, sterowaniu wymuszonym dynamiką lub sterowaniu ślizgowym. Opracowane „algorytmy energooszczędnego sterowania" są łatwe do wdrożenia cyfrowego i mogą być stosowane do sterowania położeniem istniejących napędów prądu zmiennego.

[1]University of Žilina, Faculty of Electrical Engineering, Department of Power Electrical Systems, Veľký Diel, 01026 Žilina, SLOVAKIA, phone: +421 041 513 2155, email: Peter.Minarech@kves.uniza.sk, Jan.Vittek@fel.uniza.sk
[2]Technical University of Radom, Faculty of Transport and Electrical Engineering, POLAND; Radom 26-600; Malczewskiego 29, phone: +48 48 361-77-00, email: e.szychta@pr.radom.pl, m.luft@pr.radom.pl.

1. INTRODUCTION

Savings in electrical energy consumption can limit carbon footprint and bring profit to the environment. New types of controller for electrical motors (*rotating and linear*) can help to save substantial part of energy consumed on position maneuver. Contribution of this paper is development of energy saving control algorithms suitable for all position controlled servo-systems. Implementation of such algorithms can bring energy savings for the drive with currently used inverter and machine.

As a verification of possible energy savings a state-space based closed-loop position control system with prescribed dynamics, [1] has been investigated with the aim to minimize energy demands in position applications. An energy consumption of the PMSM for position maneuvers lasting T=0,5 s and applied position demand, θ_{rd}=10 rad was recorded for varying prescribed settling times of position response $T_{ss} \in (50 - 250)$ ms as shown in Fig.1. During position maneuver at t=0,25 s the drive was loaded with nominal torque, T_{nom} =8 Nm.

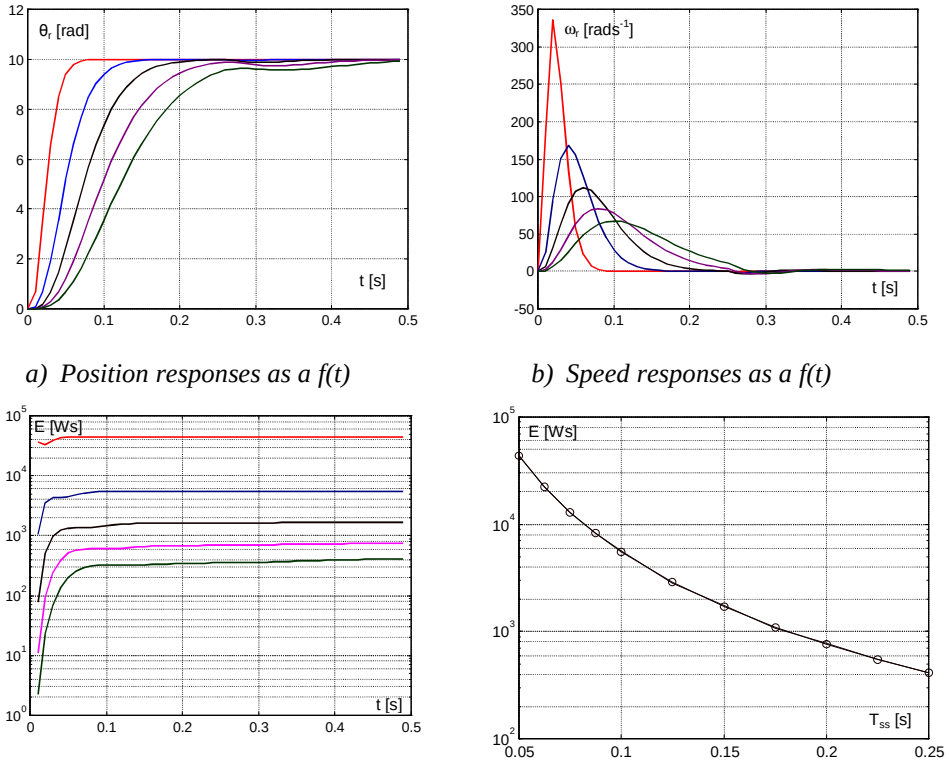

a) Position responses as a f(t)

b) Speed responses as a f(t)

c) Total consumed energy as a function of time

d) Consumed energy as a function of settling time, T_{ss} , B=0,05 kgm^{-2}s^{-1}

Fig. 1. Energy demands for state-space position control and various settling times

Subplot a) shows chosen individual position responses as functions of time while subplot b) shows corresponding rotor velocities as the same function. Total energy consumption as a logarithmic function of time is shown in subplot c). Total energy consumption for whole position maneuver as a logarithmic function of prescribed settling time is summarized in subplot d) together with its polynomial regression curve.

Approximation with eighth order polynomial was exploited to gain expression for energy demand as a function of prescribed settling time. For the energy demand of the drive without viscous friction this polynomial has form:

$$w = 10^{12}(3{,}0385t^8 - 3{,}8333t^7 + 2{,}0769t^6 - 0{,}6315t^5 + 0{,}1180t^4 - 0{,}0139t^3 + 0{,}001t^2,$$

and if viscous friction B=0,05 $kgm^{-2}s^{-1}$ is taken into account then the approximation polynomial has form:

$$w = 10^{12}(3{,}0581t^8 - 3{,}857t^7 + 2{,}0892t^6 - 0{,}635t^5 + 0{,}1186t^4 - 0{,}014t^3 + 0{,}001t^2, \text{ [Ws, s]}.$$

From energy saving point of view these results clearly demonstrate that the slowest position response with lowest angular speed has lowest energy demands. ***In general it can be concluded that for energy saving control the maximum speed of the electric drives should be kept to the minimum practicable values***.

To decrease energy demands for defined position maneuver time the '*minimum energy generator' i*s developed. This generator computes a velocity-time profile with minimal cruising speed together with corresponding position reference. Generator also respects Coulomb friction of the machine. Computed acceleration, velocity and position profiles limit energy consumption for given rotor position request and specified maneuver time. Results of position control were verified by simulation and experimentally with good agreement with theoretical predictions.

2. CONTROL SYSTEM DEVELOPMENT

2.1 Mathematical model of PMSM

Equations of the mathematical model of PMSM are formulated in *dq0* coordinate system coupled with the rotor, where:

$$\Psi_d = L_d i_d + \Psi_{PM}, \tag{1}$$

$$\Psi_q = L_q i_q, \tag{2}$$

are linkage magnetic flux components,

$$\frac{di_d}{dt} = \frac{1}{L_d}\left(u_d - R_s i_d + \omega_r L_q i_q\right), \tag{3}$$

$$\frac{di_q}{dt} = \frac{1}{L_q}\left(u_q - R_s i_q - \omega_r L_d i_d - \omega_r \Psi_{PM}\right), \tag{4}$$

are stator currents differential equations. Electrical torque of the motor is done as:

$$\Gamma_e = \frac{3p}{2}\left(\Psi_d i_q - \Psi_q i_d\right). \tag{5}$$

For vector control of PMSM up to nominal speed, where conditions $i_d = 0$ is kept, the equation for electric torque can be simplified as:

$$\Gamma_e = \frac{3p}{2}\left(\Psi_{PM} i_q\right). \tag{6}$$

Angular speed, ω_r and angle of the rotor, θ_r as mechanical state-variables are described as:

$$\frac{d\omega_r}{dt} = \frac{1}{J}\left(\Gamma_e - \Gamma_L\right), \tag{7}$$

$$\frac{d\theta_r}{dt} = \omega_r . \tag{8}$$

2.2 General concept of energy saving position control system

The goal of a new concept of position control is to create control system satisfying conditions for energy savings. Its basic concept as digitally controlled a.c. drive with prescribed position dynamics is shown in Fig. 2. The input of the control diagram is demanded position and rotor position is controlled output. Overall position control system, usually of cascade structure, can be based on principles of field oriented control (FOC), sliding mode control (SMC), forced dynamics control (FDC) or any other position control algorithm.

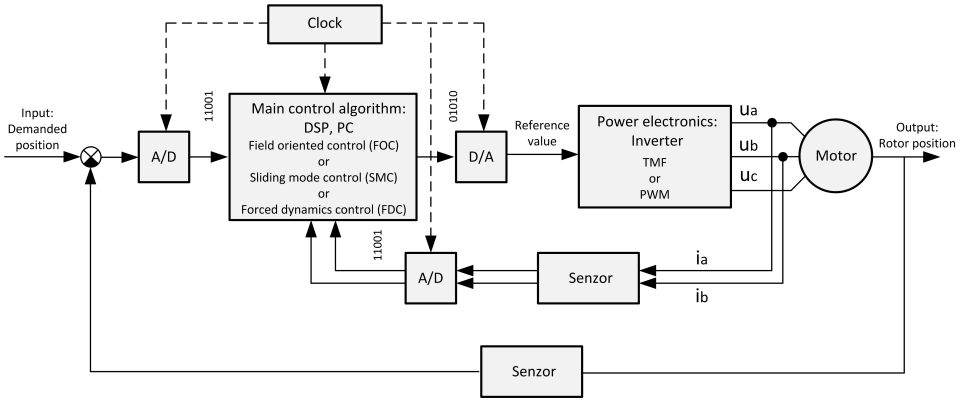

Fig.2. Overall position control system for AC drives

As it was shown, the best strategy of energy saving position control requires an algorithm, which for a given position maneuver minimizes the drive's velocity. Practical solution satisfying this theory is trapezoidal speed profile, which produces constant cruising speed. It is highly desirable if acceleration profile, which corresponds to this speed profile,

takes into account load torque. This means that the magnitude and time of the acceleration or deceleration is varying such a way, that a new position control algorithm is saving energy and load torque is completely compensated. Concept of the *'overall position control algorithm'* for energy saving control is shown in the Fig. 3.

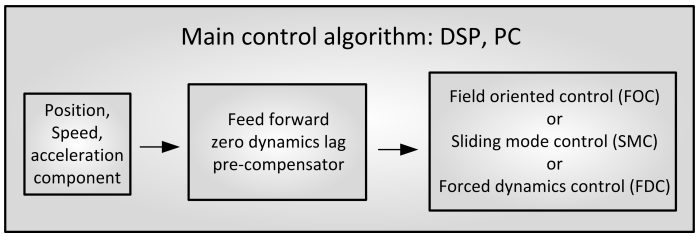

Fig.3. Concept of the main control algorithm for energy saving position control

Complete block diagram of energy saving position control is shown in Fig. 4. It consists of position control system of Fig. 2, which is completed with '*generator of energy saving position profile*' and '*zero dynamics lag precompensator*'.

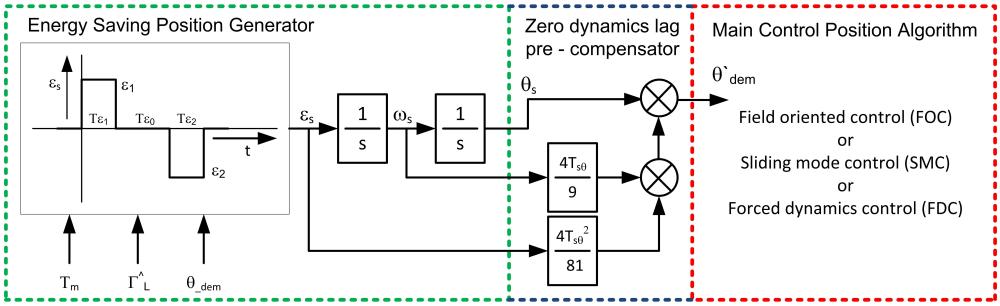

Fig.4. Overall energy saving position control system block diagram

2.3 Main Position Control Algorithm with PD Controller

Designed position control system has a nested structure. Inner speed control loop exploits principles of FDC and its response is assumed in the form of the first order delay.

$$F(s)=\frac{\dot{\theta}_r(s)}{\dot{\theta}_{r\,dem}(s)}=\frac{\omega_r(s)}{\omega_{r\,dem}(s)}=\frac{1}{1+sT_\omega}, \tag{9}$$

where T_ω is prescribed settling time of the inner speed control loop.

If position control system is to have a specified settling time, $T_{s\theta}$, then the desired second order transfer function may be determined with the aid of the settling time formula, [1]:

$$\frac{\theta_r(s)}{\theta_{r\,dem}(s)} = \left[\frac{1}{1 + s\frac{T_{s\theta}}{1{,}5(1+n)}}\right]^n\Bigg|_{n=2} = \frac{\frac{81}{4T_{s\theta}^2}}{s^2 + \frac{9}{T_{s\theta}}s + \frac{81}{4T_{s\theta}^2}}. \tag{10}$$

Converting (10) into time domain yields the second order closed loop differential equation for the rotor position:

$$\ddot{\theta}_r = \frac{81}{4T_{s\theta}^2}\left(\theta_{r\,dem} - \theta_r\right) - \frac{9}{T_{s\theta}}\dot{\theta}_r. \tag{11}$$

Equating the right hand sides of (9) and (11) and solving the equation for the control variable, $\dot{\theta}_{r\,dem}$, then yields the following FDC law:

$$\dot{\theta}_{r\,dem} = \left(1 - \frac{9T_\omega}{T_{s\theta}}\right)\dot{\theta}_r + \frac{81T_\omega}{4T_{s\theta}^2}\left(\theta_{r\,dem} - \theta_r\right). \tag{12}$$

The resulting block diagram for rotor position closed-loop control is shown in Fig. 5.

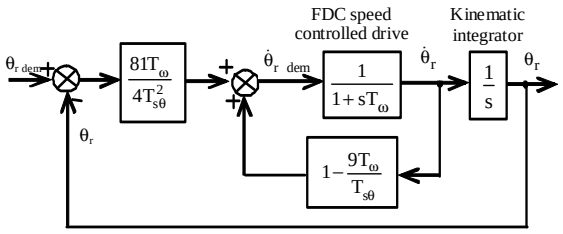

Fig. 5. Block diagram for FDC of rotor angle

Such design of position control system allows arbitrary choice of time constants, T_ω and $T_{s\theta}$ for speed and position control loop.

2.4 Zero dynamics lag pre-compensator

For better tracking of time varying position input derivative precompensator can contribute to the improvements of the designed position control system performance. Precompensator compensates the dynamic lag between the continuously varying model output and the actual rotor position so that the motion of the real mechanism is '*slaved*' through being precisely to that of the model. The precompensator has the inverse closed-loop transfer function to the plant equation (10) with unity d.c. gain and thus:

$$F_{PC}(s) = \frac{\theta_{mod}(s)}{\theta_m(s)} = s^2\frac{4T_s^2}{81} + s\frac{4T_s}{9} + 1. \tag{13}$$

2.5 Generator of energy saving position profile

The best position control strategy to save energy is in minimizing the drive's velocity for a given position maneuver. There are many different speed profiles, which can achieve demanded position at specified settling time. To minimize viscous friction losses, which are proportional to the velocity, rectangular acceleration profile is exploited for computation of cruising speed, $\omega_{cr}(t)$ and position profiles, $\theta(t)$ are produced by subsequent integration of the prescribed acceleration as it is shown in Fig. 5a. Demanded acceleration and deceleration without taking into account load torque is defined by (14), where J is moment of the drive's inertia and $\Gamma_{el\,max}$ is maximum electric torque of the machine and Γ_{FC} is coulomb friction determined by measurement.

$$\varepsilon_m = \frac{\Gamma_{el\,max} - \Gamma_{FC}}{J} \tag{14}$$

If load torque is taken to the account the acceleration and deceleration equation is as:

$$\varepsilon_{mi} = \frac{\Gamma_{el\,max} - \Gamma_{FC} \mp \Gamma_L}{J}, i = 1,2 \tag{15}$$

Moreover, chosen trapezoidal speed profile, which takes into account load torque, shown in Fig. 5b yields lower energy expenditure for a specified maneuver time then conventional linear control techniques and it has a precisely defined and truly finite settling time [3].

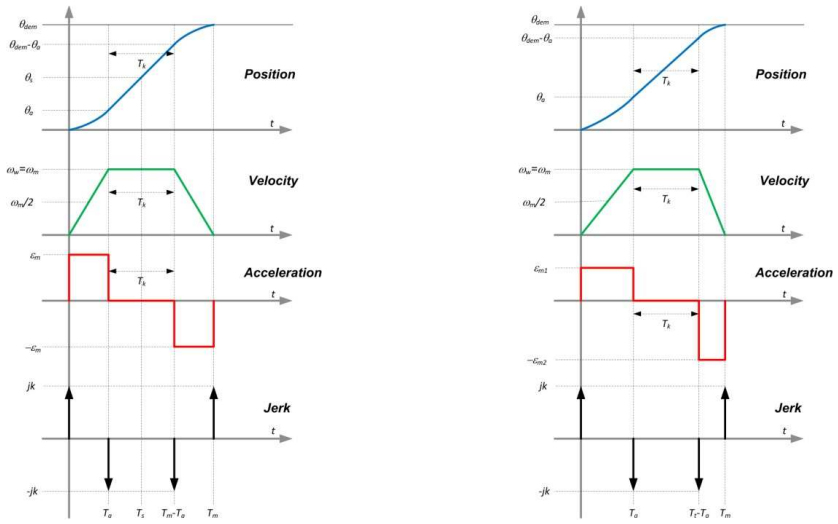

Fig.5. Minimum energy generator profiles, a) without and b) with taking into account active load torque Γ_L

If demanded rotor position, θ_{dem}, total maneuver time, T_m and magnitude of acceleration, ε_{m1} and deceleration, ε_{m2} are known, following formula (16) determines cruising velocity, ω_{cr} for position maneuver:

$$\omega_{cr} = \frac{1}{2} k_\varepsilon T_m \left[1 - \sqrt{1 - \frac{4\theta_{dem}}{k_\varepsilon T_m^2}} \right], \tag{16}$$

where coefficient k_ε is defined as:

$$k_\varepsilon = \frac{2\varepsilon_{m1}\varepsilon_{m2}}{\varepsilon_{m1} + \varepsilon_{m2}}. \tag{17}$$

Condition for reaching of cruising speed is as follows:

$$\varepsilon_{m1} T_{\varepsilon 1} = \varepsilon_{m2} T_{\varepsilon 2}. \tag{18}$$

Using condition (18) time of acceleration $T_{\varepsilon 1}$ and deceleration $T_{\varepsilon 2}$ is as follows:

$$T_{\varepsilon i} = \frac{T_m k_\varepsilon}{2\varepsilon_{mi}} \left[1 - \sqrt{1 - \frac{4\theta_{dem}}{k_\varepsilon T_m^2}} \right]. \tag{19}$$

If shortest maneuver time requires full torque of the motor for acceleration and deceleration interval while interval for cruising speed drops to zero then conditions for '*near-time optimal control*' are satisfied.

3. CALCULATION OF ENERGY CONSUMPTION

3.1 Input power

Calculation of energy consumption results from the first and second law of thermodynamics known as the law of energy degradation. All of the energy that enters the motor is equal to the energy on the shaft of the motor plus reversible and irreversible energy components.

Total input power P_{in} to the machine in terms of (a,b,c), (α,β) stationary variables and (d,q) rotating variables is:

$$P_{in} = u_a i_a + u_b i_b + u_c i_c = \frac{3}{2}\left(u_\alpha i_\alpha + u_\beta i_\beta\right) = \frac{3}{2}\left(u_d i_d + u_q i_q\right). \tag{20}$$

Total energy expenditure, E_E is calculated as time integral of input power, P_{in} :

$$E_E = \int_0^{Tm} P_{in} dt, \tag{21}$$

where T_m is maneuver time.

There are two major components of energy that leave the motor, a) the energy supplied to the connected load and b) the heat that escapes to the surrounding space. In additions, to these there is the energy of vibration and noise, or acoustic energy.

3.2 Reversible energy

A reversible process is defined as one for which the system and surroundings can be completely restored to the respective initial states after a process has occurred [4]. The gain in reversible energy would be in the form of:

1) Kinetic energy of rotation (stored in rotor inertia, J):

$$E_{kin} = \frac{1}{2} J\omega^2 . \tag{22}$$

2) Energy stored in magnetic field:

$$E_{mag} = \frac{1}{2}\left(L_s i_a^2 + L_s i_b^2 + L_s i_c^2\right) = \frac{3}{4}\left(L_d i_d^2 + L_q i_q^2\right). \tag{23}$$

3.3 Irreversible energy

The irreversible energy of the motor would be one which raises its temperature, i.e., heat resulting from electrical winding losses and magnetic core losses as well as from friction. Stator joule losses can be calculated for phase variables as:

$$\Delta P_{js} = R_s i_a^2 + R_s i_b^2 + R_s i_c^2 \tag{24}$$

and similar way for (α_β) and (d_q) coordinate systems.

Input energy, changed into heat in stator resistances is calculated as follows:

$$E_{Pjs} = \int_0^{Tm} \left[P_{js}\right] dt \tag{25}$$

Mechanical losses, ΔP_{mech} are the sum of viscous, $\Delta P_{Viscous}$ and coulomb, $\Delta P_{Coulomb}$ frictions, where B is coefficient of viscous friction and X is the ratio of coulomb friction to nominal torque:

$$\Delta P_{mech} = \Delta P_{Viscous} + \Delta P_{Coulomb} = \left(B\omega + X\Gamma_{el}\right)\omega . \tag{26}$$

Energy spend on mechanical losses can be then determined as:

$$E_{\Delta P_{mech}} = \int_0^{Tm} \left[\Delta P_{mech}\right] dt \tag{27}$$

Then total power supplied to the load consists of power required to cover load torque at the speed of the drive and mechanical losses (28):

$$P_{Total_{\Gamma L}} = P_{\Gamma_L} + \Delta P_{mech} + J\omega\frac{d\omega}{dt}, \tag{28}$$

where P_{mech} is input mechanical power and ΔP_{mech} are mechanical losses.

Energy supplied to the connected load, $E_{PTotal\Gamma L}$ can be calculated as:

$$E_{P_{Total_{\Gamma z}}} = \int_0^{Tm} \left[P_{Total_{\Gamma z}}\right] dt \tag{29}$$

4. VERIFICATION OF CONTROL ALGORITHM BY SIMULATION

For simulation and also experimental verification PMSM with parameters described in Appendix has been used. Energy expenditure of two types of position control *(step response and energy saving algorithms)* of PMSM are compared. Position change request was set to θ_{dem}=18,85 rad *(3 revolutions*) for fixed maneuver time T_m=0,2 *s*. Coefficient, B=0,002 $kgm^{-2}s^{-1}$ was used to include losses due to viscous friction.

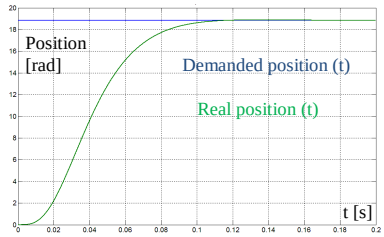

a1) Position as a function of time

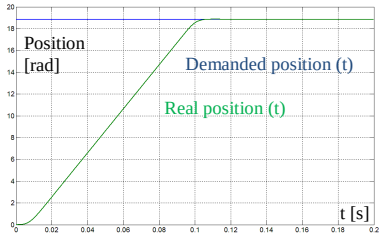

a2) Position as a function of time

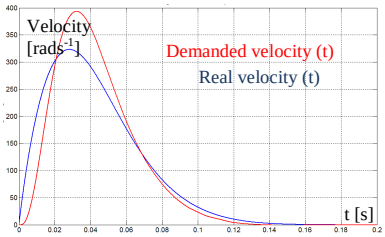

b1) Velocity as a function of time

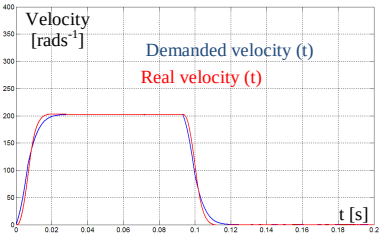

b2) Velocity as a function of time

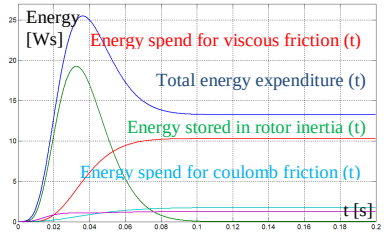

c1) Energy consumption as a function of time

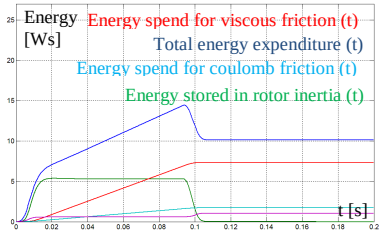

c2) Energy consumption as a function of time

Fig.6 Position and speed response with corresponding energy consumption of 1) step position demand and 2) energy saving control algorithm

Fig. 6 shows as subplots a) and b) position and speed responses respectively together with energy consumption in subplot c) for step response to the demanded position marked with index 1) while subplots marked with index 2) show in the same functions for energy saving control algorithm. Total energy consumption of step response control algorithm was $E_{P\ Total}$=13,25 Ws and for energy saving control algorithm it was $E_{P\ Total}$=10,12 Ws.

In spite of the same maneuver time energy saving control algorithm with reduced cruising speed for a given position change has 23,6% lower energy consumption if

compared with step response. The analysis of energy components shows that in spite of the same coulomb friction for both algorithms the viscous friction is higher for the step response algorithm due to its direct proportion to the drive's velocity

5. EXPERIMENTAL VERIFICATION

Experiments has been performed with 32-bit digital signal controller MPC5567, a member of the MPC5500 family of microcontrollers built on the '*power architecture embedded technology*' including floating point. Laboratory bench is shown in Fig. 7.

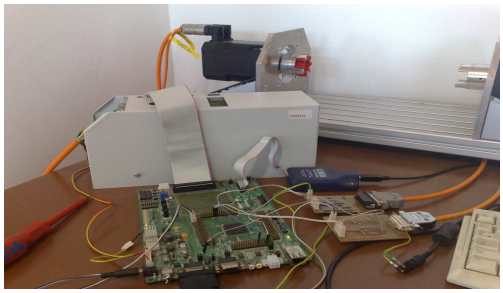

Fig. 7. Laboratory bench for evaluation of energy consumption: 1. 32-bit DSC with floating point, 2. voltage converter, 3. drive with –PMSM, 4. resolver interface

Voltage converter controlled by MPC5567 produces modulation voltages for PMSM. Experimental results for change request of position was again set to θ_{dem}=18,85 rad (*3 revolutions*) with starting time at t_s=0,2s and end of motion at t_e=0,4s, to keep the same time interval as for simulations.

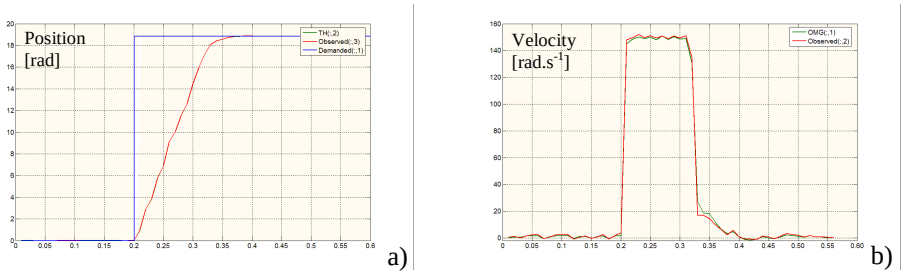

a) b)

Fig. 8. Experimental results for energy saving control algorithm, a) demanded and real position response, b) real and observed velocity

6. CONCLUSIONS

Presented simulation results confirmed that a new energy optimal position control algorithm can save a significant proportion of drive's input energy. Described control algorithms are based on acceleration, speed and position profile generation. Feed-forward precompensator is exploited for better tracking of generated time varying position.

Acceleration, cruising speed and deceleration for a new energy saving algorithm complies to the prescribed time of position maneuver. This way the velocity of the drive is reduced and therefore less energy is dissipated during position maneuver. Simulation results confirm that proposed control algorithm can bring savings of input energy if compared with step response position control. Experimental results confirmed that a new energy saving position control algorithm can be easily digitally implemented into control system of existing servo-drives.

7. REFERENCES

[1] S.J. Dodds, *Settling time formulae for the design of control systems with linear closed loop dynamics*, in Proc. of the int. conf. AC&T - Advances in Computing and Technology, University of East London, United Kingdom, 2007.

[2] Dodds, S. J.: *Sliding Mode Vector Control of PMSM Drives with Minimum Energy Position Following*, Proceedings of EPE-PEMC conf., 2008, Poznan, Poland pp. 2559-2566.

[3] Vittek, J., Briš, P., Skalka, I., Filka, R., Minárech, P., Faber, J.: *Experimental Verification of Energy Saving Position Control Algorithm Applied to the Drives with PMSM*, EPE-PEMC 2010, 14th Int. Power Electronics and Motion Control Conf. Ohrid, Macedonia, 2010, 09, 6-8, AFC, str.: S10-1 - S10-6, 978-1-4244-7854-5

[4] Wiley, J.: „ *Modeling and high-performance control of electrical machines* ” , John Wiley & Sons, New Jersey, ISBN: 0-471-68449-X.

[5] Saari, J.: „ *Thermal analysis of high-speed induction machines* ”, Acta Polytechnica Scandinavica – Electrical Engineering Series No. 90, Helsinki University of Technology, Finland, ISBN 952-5148-43-2.

[6] Dodds, S. J., Sooriyakumar, G., Perryman, R.: *Minimum Energy Forced Dynamics Control of PMSM*. Proc. of the 3rd IASME/WSEAS Int. conf. on Energy & Environment, Cambridge, United Kingdom, pp.: 173-179.

[7] Arevalo, V.M., Opticos, A., Ensenada, B.C.: *Sinusoidal Velocity Profiles for Motion Control*, Mexico 22830.

[8] Minárech, P., Vittek, J.: *Energy Demands of the Position Drives employing PMSM Control by Forced Dynamics*, University of Žilina, ISBN: 978-80-554-0196-6.

APPENDIX

PMSM parameters: rated power P_N=1440 W, rated current I_N=3,64 A, rated voltage U_N=330 V, rated speed n_N=3000 min^{-1}, rated torque M_N=4,6 Nm, no. of pole-pairs p=5, R_{2ph}=2,627 Ω, L_{2ph}=26,66 mH, Ψ_{PM}=0,13 Wb, moment of inertia J=2,6 $kg.cm^2$, torque constant K_m=1,376 Nm/A.

ACKNOWLEDGMENT

The authors wish to thank for the support to the Slovak grant Agency VEGA for funding project V-11-023-00 and R&D operational program Centre of Excellence of Power Electronics Systems and Materials for their Components. The project is funded by European Community, ERDF – European Regional Development Fund.